UC Irvine
UC Irvine Previously Published Works

Title

Can surface pressure be used to remove atmospheric contributions from GRACE data with sufficient accuracy to recover hydrological signals?

Permalink

https://escholarship.org/uc/item/58b7f341

Journal

Journal of Geophysical Research, 106(B8)

ISSN

0148-0227

Authors

Velicogna, Isabella
Wahr, John
Van den Dool, Huug

Publication Date

2001-08-10

DOI

10.1029/2001jb000228

Copyright Information

Peer reviewed

Can surface pressure be used to remove atmospheric contributions from GRACE data with sufficient accuracy to recover hydrological signals?

Isabella Velicogna and John Wahr

Department of Physics and Cooperative Institute for Research in Environmental Science, University of Colorado, Boulder, Colorado USA

Huug Van den Dool

Climate Prediction Center, National Centers for Environmental Prediction, Washington., D.C., USA

Abstract. The Gravity Recovery and Climate Experiment (GRACE) satellite mission will resolve temporal variations in gravity orders of magnitude more accurately and with considerably higher resolution than any existing satellite. Effects of atmospheric mass over land will be removed prior to estimating the gravitational field, using surface pressure fields generated by global weather forecast centers. To recover the continental hydrological signal with an accuracy of 1 cm of equivalent water thickness down to scales of a few hundred kilometers, atmospheric pressure must be known to an accuracy of 1 mbar or better. We estimate errors in analyzed pressure fields and the impact of those errors on GRACE surface mass estimates by comparing analyzed fields with barometric surface pressure measurements in the United States and North Africa/Arabian peninsula. We consider (1) the error in 30-day averages of the pressure field, significant because the final GRACE product will average measurements collected over 30-day intervals, and (2) the short-period error in the pressure fields which would be aliased by GRACE orbital passes. Because the GRACE results will average surface mass over scales of several hundred kilometers, we assess the pressure field accuracy averaged over those same spatial scales. The atmospheric error over the 30-day averaging period, which will map directly into GRACE data, is generally < 0.5 mbar. Consequently, analyzed pressure fields will be adequate to remove the atmospheric contribution from GRACE hydrological estimates to subcentimeter levels. However, the short-period error in the pressure field, which would alias into GRACE data, could potentially contribute errors equivalent to 1 cm of water thickness. We also show that given sufficiently dense barometric coverage, an adequate surface pressure field can be constructed from surface pressure measurements alone.

1. Introduction

Most modern, high-precision geodetic measurements of time variable processes can benefit from accurate knowledge of atmospheric pressure. For example, precise space-based positioning methods (e.g., Global Positioning System (GPS), very long baseline interferometry, satellite laser ranging, and sea surface altimetric heights) require estimates of surface pressure and temperature to model the dry air contribution to the signal delay [e.g., *Rocken et al.*, 1993]. The Earth's elastic response to loading by atmospheric pressure can cause vertical crustal displacements of up to 5 mm [e.g., *Van Dam et al.*, 1994], and the direct attraction of the atmosphere can cause surface gravity signals of several μGals [*Neibauer and Faller*, 1992], both of which can contaminate estimates of tectonic motion. Accurate knowledge of the atmospheric mass distribution will be particularly important for the coming new generation of satellite gravity missions and especially for the Gravity Recovery and Climate Experiment (GRACE). At scales $\geq$ 300 km, error in the atmospheric correction will likely dominate the error in GRACE measurements of time variable gravity over land.

GRACE, under the joint sponsorship of NASA and the Deutsches Zentrum fur Luft und Raumfahrt (DLR),

is scheduled for a 2001 launch with a nominal 5-year lifetime. GRACE will consist of two satellites in low Earth orbit (an initial altitude of 450-500 km) that range to each other across a few hundred kilometers of separation using microwave phase measurements. Onboard GPS receivers will determine the position of each spacecraft in a geocentric reference frame. The geoid estimate will combine the GPS location with ranging information and subtract out nongravitational accelerations measured by onboard accelerometers. The resulting data will map the gravity field orders of magnitude more accurately and to considerably higher spatial resolution than any existing satellite.

GRACE will resolve temporal variations in gravity at length scales of a few hundred kilometers and larger, with accuracies of better than 1 cm of equivalent water thickness over land and of a few tenths of a millibar or better in ocean bottom pressure and will produce a complete global map once every 30 days. Temporal variations in gravity can be used to study a large number of problems in several disciplines, from monitoring changes in water, snow, and ice on land to determining changes in ocean bottom pressure to studying postglacial rebound (PGR) of the solid Earth. Comprehensive descriptions of these and other applications are given by *Dickey et al.* [1997] and *Wahr et al.* [1998]. Contamination from the changing distribution of atmospheric mass will be the limiting error source for estimating changes in continental water storage at wavelengths greater than ~300 km [*Wahr et al.*, 1998].

Analyzed atmospheric fields will be used to remove the effects of the atmosphere over land from GRACE measurements prior to constructing the spherical harmonic coefficients of the geoid, which will be the GRACE final product. However, there will be errors in those fields which will then map into errors in GRACE residual hydrological estimates. The global RMS of monthly variation in continental hydrology is typically 3 cm of water and, locally, can be as much as 15 cm of water when averaged over circular areas of 300-km radius. In order to recover the continental hydrological signal with an accuracy of 1 cm of equivalent water thickness the atmospheric pressure needs to be known to an accuracy of 1 mbar (i.e., the atmospheric mass needed to generate 1 mbar of pressure at the Earth's surface is equivalent to the mass of 1 cm of water) [*Dickey et al.*, 1997]. The atmospheric correction will not be applied to GRACE data over the oceans for reasons discussed by *Wahr et al.* [1998], although the atmospheric pressure will be used (along with winds) to force the barotropic ocean model that will generate the combined bottom pressure effect for the ocean areas. However, in applications where both GRACE data and altimetric sea surface height are to be assimilated the atmospheric mass correction will have to be applied postprocessing to either the geoid or, more probably, the altimetric heights.

The main purpose of this paper is to estimate reliably the errors in analyzed pressure fields, which we

approach by comparing to barometric measurements of surface pressure. *Wahr et al.* [1998] simulated errors in the pressure fields by taking the difference between 30-day averages of the pressure fields generated by the European Centre for Medium-Range Weather Forecasts (ECMWF) and those generated by the National Centers for Environmental Prediction (NCEP) and dividing that difference by $\sqrt{2}$ under the assumption that the fields are about equally accurate and that errors are uncorrelated. In fact, the ECMWF and NCEP pressure fields are likely to have errors in common, and these would not be included by *Wahr et al.*'s [1998] ECMWF/NCEP differences. To provide continuity with the previous analysis [*Wahr et al.*, 1998], when comparing the two analyzed fields in this paper, we divide the difference of the two by $\sqrt{2}$ and describe the comparison as RMS error. Comparisons between measurements and analyzed fields (without the $\sqrt{2}$ factor) will be refered to as RMS difference. Our analysis assumes that all atmospheric mass variations occur in an infinitely thin layer at the Earth's surface, ignoring the effects of the vertical mass distribution. S. Swenson and J. Wahr (Estimated effects of the vertical distribution of atmospheric mass on time-variable gravity, submitted to *Journal of Geophysical Research*, 2000) show that the thin layer assumption introduces errors into GRACE estimates of surface mass with RMS <1.0 mm of equivalent water thickness when averaged over all latitudes (though RMS differences at some high-latitude locations can be as large as 2-4 mm). Also, our analysis implicity assumes that barometric measurements have negligible error. In the discussion in section 5 we will show that this is a reasonable assumption.

We examine how well the ECMWF and NCEP/National Center for Atmospheric Research (NCAR) Reanalysis models reproduce barometric measurements of surface pressure in two regions: the United States and North Africa/Arabian peninsula (Figure 1). Both regions have areas of low and high topographic relief, but whereas the United States has numerous high-quality barometric observations, pressure measurements in North Africa/Arabian peninsula are sparser and have more temporal gaps and more and larger outliers. We consider Egypt and the Arabian peninsula because both have been proposed as focus regions for verification of GRACE accuracy because of their extremely low precipitation and relatively simple hydrologic systems. The United States represents a best case scenario for observational constraint of surface pressure, while the distribution of pressure measurements in North Africa/Arabian peninsula is more typical of the global coverage.

When estimating the effects of atmospheric pressure errors on GRACE, it is useful to separate those errors into two components: (1) errors averaged over 30-day intervals, which are relevant because GRACE will average measurements collected over 30-day periods to produce geoid maps, and (2) short-period pressure errors,
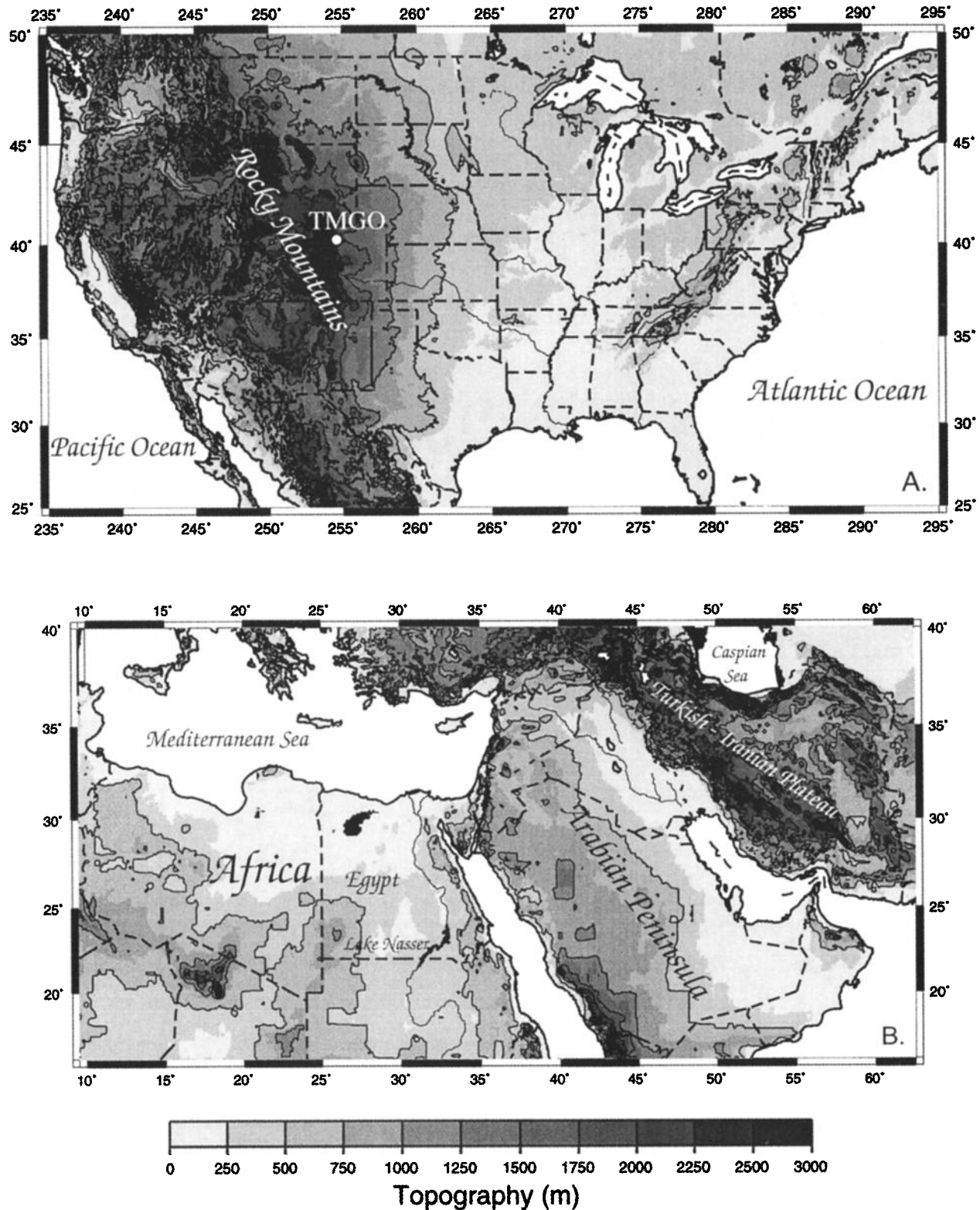
Figure 1. Location map depicting topography of the two studied areas: (a) United States, and (b) North Africa/Arabian peninsula.

which will be undersampled by GRACE orbital passes and hence will not average out entirely. In this paper we will consider both components of the final error. A secondary objective of this paper is to verify whether or not an accurate surface pressure field can be constructed from surface pressure measurements alone.

2. Preliminaries

To motivate this analysis, we first describe the characteristics of GRACE data and how these data will likely be used to estimate surface mass variability. We also discuss here the data sets used in this paper.

2.1. Spatial Averaging

The Earth's global gravity field is commonly described in terms of the shape of the geoid: i.e., the equipotential surface corresponding to mean sea level over the oceans. The geoid can be expanded in a spherical harmonic representation as [Kaula, 1966]

$$N(\theta, \phi) = a \sum_{l=0}^{\infty} \sum_{m=-l}^{l} \tilde{P}_{lm}(\cos\theta)\{C_{lm} \cos m\phi$$
$$+ S_{lm} \sin m\phi\}, \qquad (1)$$

where a is the Earth's mean radius, θ and ϕ are colatitude and east longitude, C_{lm} and S_{lm} are dimensionless coefficients, and $\tilde{P}_{lm}$ is the normalized associated Legendre function [e.g., Chao and Gross, 1987].

Once every 30 days, GRACE will provide a geoid model (i.e., numerical values for C_{lm} and S_{lm}) up to degree and order (l and m) of ~100, corresponding to spatial scales (i.e., half wavelengths) of ~200 km and greater. Changes in C_{lm} and S_{lm} are related to changes in the Earth's density distribution $\Delta\rho(r, \theta, \phi)$ via [Chao and Gross, 1987; Chao et al., 1987]:

$$\begin{Bmatrix} \Delta C_{lm} \\ \Delta S_{lm} \end{Bmatrix} = \frac{3}{4\pi a \rho_{\text{ave}}(2l+1)} \int \Delta\rho(r, \theta, \phi)$$
$$\cdot \tilde{P}_{lm}(\cos\theta) \left(\frac{r}{a}\right)^{l+2} \begin{Bmatrix} \cos m\phi \\ \sin m\phi \end{Bmatrix}$$
$$\cdot \sin\theta \, d\theta \, d\phi \, dr, \qquad (2)$$

where ρ_{ave} (=5517 kg/m^3) is the average density of the Earth and ΔC_{lm} and ΔS_{lm} are changes in the spherical harmonic coefficients of the geoid.

Suppose that $\Delta\rho$ is concentrated in a thin layer of thickness H at the Earth's surface, which should be thick enough to include those portions of the atmosphere, oceans, ice caps, and belowground water storage with significant mass fluctuations. H thus approximately corresponds to the thickness of the atmosphere and is of the order of 10-15 km. Note that because of the radial integral in (2), GRACE will be unable to resolve mass anomalies at different radial positions and so will be incapable of distinguishing between water on the surface, in the soil, or in subsoil layers and will also be unable to discriminate between water, snow, ice, or atmospheric mass variations. This is the reason that variations in atmospheric mass will contaminate estimates of continental water storage (if the latter are to be measured by GRACE and the former cannot be accurately eliminated).

Because H is much less than the shortest spatial scale provided by GRACE, the factor $(r/a)^{l+2}$ in (2) can be approximated as 1, so that ΔC_{lm} and ΔS_{lm} can be related to the change in surface mass density $\Delta\sigma(\theta, \phi) = \int_{\text{thinlayer}} \Delta\rho(r, \theta, \phi) \, dr$. That relation can be inverted to give $\Delta\sigma$ in terms of the ΔC_{lm} and ΔS_{lm} values, using (14) of Wahr et al. [1998].

In principle, an estimate of $\Delta\sigma$ at any individual point (θ, ϕ) requires knowledge of the ΔC_{lm} and ΔS_{lm} values at all wavelengths. However GRACE will deliver 30-day coefficients only up to about l=100, and the accuracy of those coefficients will decrease rapidly with increasing l, so that pointwise estimates of $\Delta\sigma$ would be too inaccurate to be useful. Instead, GRACE will accurately deliver spatial averages of surface mass over regions of a few hundred kilometers and larger in scale. For this paper, we will follow Wahr et al. [1998] and construct the spatial average:

$$\overline{\Delta\sigma}(\theta, \phi) = \int \Delta\sigma(\theta', \phi') \, W(\gamma) \sin\theta' \, d\theta' \, d\phi', \qquad (3)$$

where γ is the angular distance between the two points (θ, ϕ) and (θ', ϕ') and $W(\gamma)$ is the normalized Gaussian function developed by Jekeli [1981] and depicted in Figure 2:

$$W(\gamma) = \frac{b}{2\pi} \frac{\exp[-b(1 - \cos\gamma)]}{1 - e^{-2b}}, \qquad (4)$$

where

$$b = \frac{\ln(2)}{[1 - \cos(r_W/a)]}. \qquad (5)$$

Here W has been normalized so that its global integral is 1, and r_W is the distance along the Earth's surface at which $W(\gamma)$ has decreased to half the value it had at $\gamma = 0$. We will refer to r_W as the averaging radius. GRACE measurements will deliver accurate estimates of $\overline{\Delta\sigma}$ for values of r_W of a few hundred kilometers and greater.

2.2. Data

The main purpose of this paper is to estimate how accurately the atmospheric contribution to the time-variable geoid can be determined. To do this, we compare analyzed surface pressure fields from ECMWF and NCEP/NCAR with surface pressure observations. We also examine the possibility of using barometric measurements alone, without any input from the pressure fields generated by global circulation models, to reproduce the surface pressure fields. To examine each of these issues, we use 6-hourly gridded global surface pressure fields from 1998, 1460 fields in all. We use NCEP/NCAR Reanalysis data, sampled on 2.5° × 2.5° global grids [Kalnay et al., 1996], and ECMWF analysis data, sampled on a global Gaussian grid spacing of 1.125° [ECMWF, 1995]. Both centers have an analysis at higher resolution; however, these data sets were not available to us and generally are not available to outside users.

The analyzed pressure fields were compared with 6-hourly barometric surface pressure measurements from the NCEP global surface observations data set. NCEP collects these data on an operational basis to serve as constraints on environmental models, and some qual-
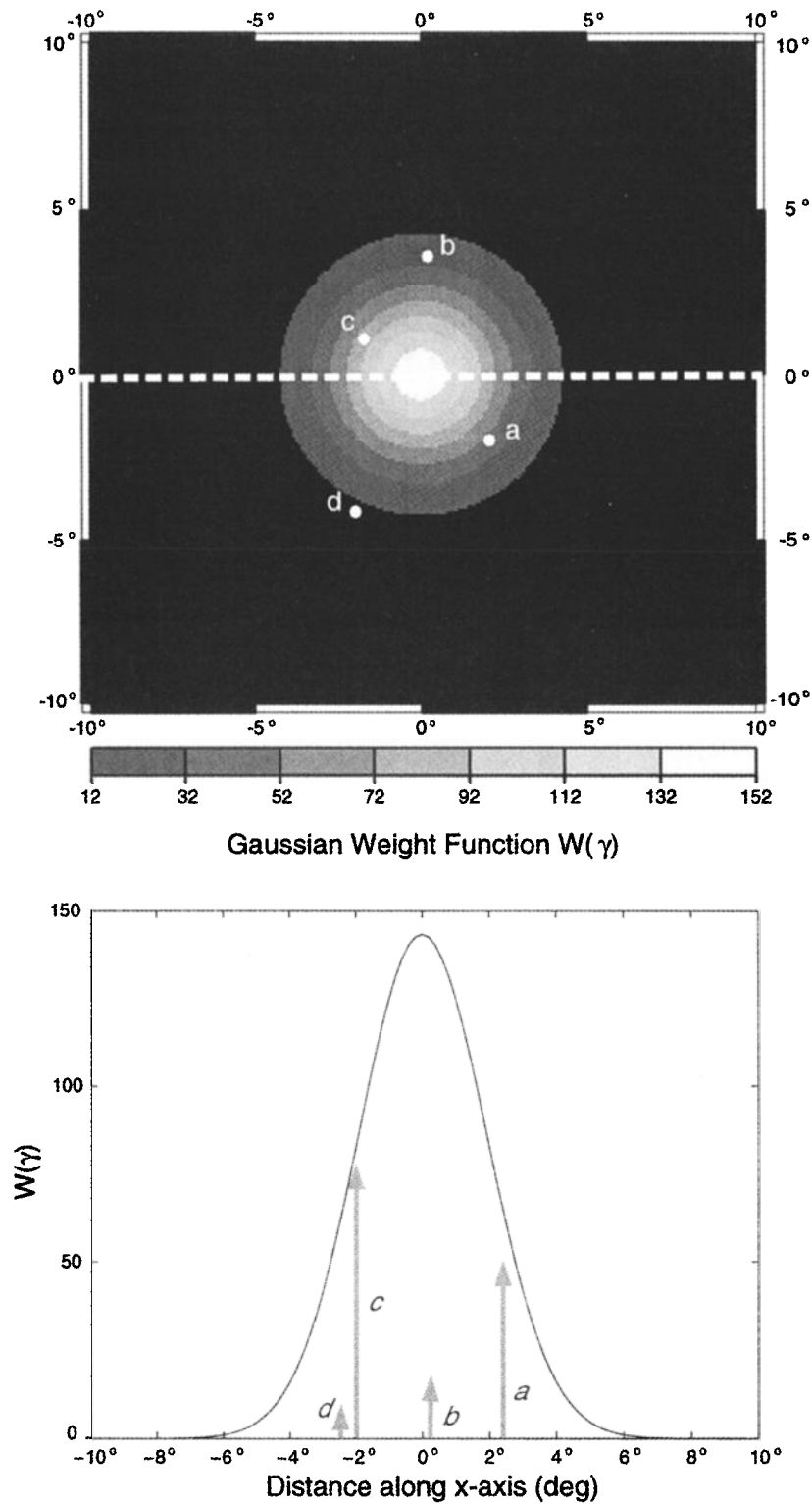
Figure 2. *Jekeli's* [1981] Gaussian weight function for radius $r_W = 250$ km: map and cross section. The cartoon depicts four observation sites below the Gaussian cap. In the cross section the shaded arrows indicate the values of $W(\gamma)$ that would weight the corresponding pressure values. The weighted sum is assigned to the center of the Gaussian.

ity control is applied. A significant problem arises in that many of these same data are also assimilated into NCEP and ECMWF global circulation models, and so the models and the observations we are comparing here are not fully independent. Consequently it is difficult to make a clear estimate of the true error in the models, but as we will demonstrate, it is possible to assign upper and lower bounds to the error. The barometeric
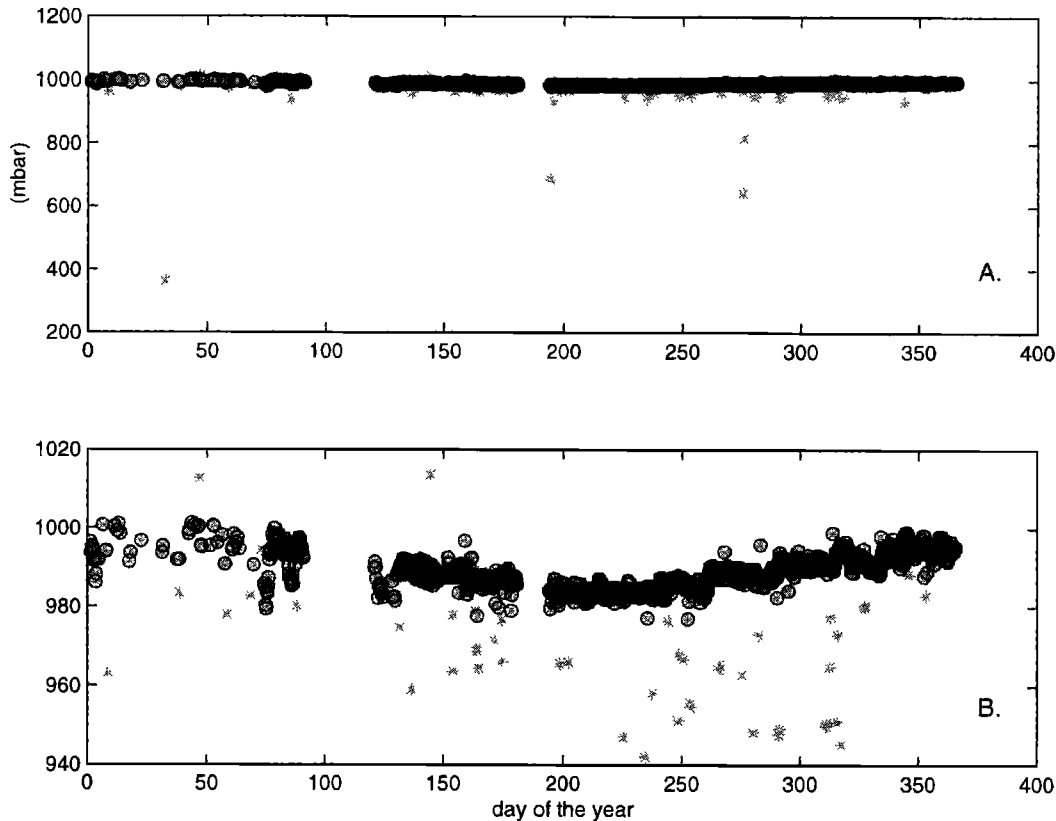
Figure 3. (a) Time series of surface pressure for the station south of Lake Nasser, Egypt. Shaded stars represent the original time series; solid circles represent the time series after outliers have been removed. (b) Detail of Figure 3a.

measurements are subject to transcription and other errors which must be addressed. We used a semivariance. analysis [*Davis*, 1986] in which the semivariance S^2 of all measurements spaced 6 hours apart was estimated from the data at a given site. Then all measurements which differed from the temporally closest measurements at $> 4S$ (99.95% confidence) were considered outliers in the pressure measurement time series and removed from the comparisons (Figure 3).

To compare the observed and analyzed surface pressure fields, we also need surface temperature and topography data for the analyzed field. For this we use ECMWF and NCEP/NCAR 6-hourly temperature and topography fields sampled on the same grid as the corresponding analyzed surface pressure fields. All data sets used in this paper were provided by the NCAR Data Support Section (DSS) archive.

As already noted, the analyzed ECMWF and NCEP/NCAR pressure fields are not independent of the surface pressure observations we will compare them with because most of the available pressure observations were assimilated into the models when constructing the analyzed fields (96% of the observations available in the United States were assimilated, and 82% in North Africa/Arabian peninsula were assimilated). Roughly speaking, the three-dimensional (3-D) multivariate atmospheric analyses made by ECMWF and NCEP incorporate observations as

$$\text{Analysis}(t) = \beta \text{ observation} (t \pm 3 \text{ hours})$$
$$+(1 - \beta) \text{ guess},$$

where t is time and the guess is a 6-hour forecast initialized using a previous analysis at $(t - 6 \text{ hours})$. Here β and $(1 - \beta)$ can be interpreted as the inverse square of the assumed error in observations and the forecast, respectively. Because different observations have different assumed errors (e.g., radiosondes are supposed to be more accurate than satellite data), the value of β is not quite unambiguous. Most centers appear to have a "global" β in the 0.3-0.5 range, in part because the real purpose of assimilating observations into these analyses is not necessarily to better describe the current state of the atmosphere but to serve as initial conditions for 10-day forecasts. Consequently, the guess field is weighted as much as or more than the observation to avoid initial "shocks" (i.e., unstable oscillations) in these forecasts.

3. Calculation of the Atmospheric Surface Pressure Error

We estimate the error in analyzed surface pressure fields from ECMWF Analysis and NCEP/ NCAR Reanalysis by comparing them with surface pressure observations. The GRACE final error will be some combination of the mean error over the 30-day averaging

period and the error from unmodeled high-frequency pressure variations that are aliased by orbital undersampling. The 30-day pressure errors will map directly into the 30-day GRACE averages. The aliasing error will depend in a complicated manner on the GRACE orbital configuration and cannot be predicted without detailed orbital simulations.

We will examine two different estimates of the error: (1) the RMS difference between model and observations averaged over 12 consecutive 30-day periods during 1998, and (2) the 6-hourly RMS difference (i.e., without time averaging) over that same year. Because the GRACE observations will spatially average the mass variations, we use the normalized averaging function W in (4) to spatially average the error. The 6-hourly RMS difference does not map directly into an error in the GRACE estimate of spatially averaged changes in surface mass because a high-frequency error in one region will not necessarily be aliased into a 30-day value over only that same region. Still, the 6-hourly RMS differences do provide some measure of the amplitude of the aliased signal. We expect our 6-hourly comparisons may overestimate the total error since the process of constructing 30-day GRACE values will presumably smooth out a significant fraction of the high-frequency contributions.

3.1. Interpolation of Analyzed Pressure to Barometer Locations

The analyzed pressure fields are defined on a regular discretization over the globe, whereas the barometer locations are irregularly spaced. For this reason we horizontally interpolate the analyzed pressure fields to the barometer locations (or vice versa) prior to calculating the RMS difference between the two. For these comparisons we will consider interpolations going both directions (i.e., (1) from the analyzed field to the barometer locations and (2) from the barometric measurements to the model grid points). To simplify the description of how the interpolation is performed, we describe here just the interpolation from analyzed pressure fields to the barometer locations. The interpolation going in the opposite direction is completely analogous.

Because the barometer is generally at a different elevation than are the nearby model grid points, the analyzed surface pressure is first adjusted to the elevation of the barometer prior to horizontal interpolation. For a given location, we assume the relationship between pressure at two different elevations, h_1 and h_2, corresponds to that of a dry, hydrostatic atmosphere and a uniform lapse rate of 0.0065 °K m^{-1} [*Haurwitz*, 1941]:

$$p_m(h_2) = p_m(h_1) \left(1 + \frac{0.0065 \mid h_1 - h_2 \mid}{T_1} \right)^{\frac{\text{sign}(h_1 - h_2)}{\alpha}},$$
(6)

where $p_m(h_i)$ is the analyzed pressure at elevation h_i, T_1 is the surface temperature at height h_1 in °K, $\alpha =$

$0.0065 R_d/g$, where g is the gravitational acceleration, and $R_d (= 287$ J K^{-1} kg^{-1}) is the gas constant for dry air.

We first reduce the pressure from the four nearest grid points of the analyzed field, A, B, C and D, from their elevations (h_A, h_B, h_C, and h_D) to the elevation h_Z of the barometer location Z using (6). Then we calculate the two-dimensional Lagrange polynomial interpolation of the four reduced values of analyzed surface pressure to the barometer location Z.

3.2. Gaussian Average of RMS Surface Pressure Differences

To simulate the signal delivered by GRACE, we calculate spatial averages using the Gaussian weighting function described in (4) and shown in Figure 2. We approximate the Gaussian average $\overline{F}_G(P)$, about the point P, of a function f defined only at a set of N discrete points, as

$$\overline{F}_G(P) = \frac{\sum\limits_{i=1}^{N} f_i W(\gamma_i)}{\sum\limits_{i=1}^{N} W(\gamma_i)},$$
(7)

where P is the center location of the Gaussian defined by $W(\gamma)$ (see (4)), γ_i is the angular distance between P and the sampled point i, $W(\gamma_i)$ is the value of the weighting function at the point i where f is defined, and N is the total number of discrete samples of f. In our case, f_i will be the difference between two different surface pressure values at the location i. This difference is most often between the observed pressure and either the ECMWF or NCEP/NCAR analyzed pressure field, interpolated to the location of the ith barometer. For comparisons of the ECMWF and NCEP/NCAR analyzed pressure fields with each other, the difference is calculated after reduction and interpolation of the NCEP/NCAR analyzed field to the ECMWF grid points. Once we have computed time series of $\overline{F}_G(P)$ for both pressure fields at a point P, we remove the yearly means from those time series and compute the RMS of the residual difference between the two. The RMS difference of Gaussian averages is evaluated at every 0.2° interval of latitude and longitude over the region of interest, using a 250-km Gaussian radius. We evaluate the RMS both for 30-day averages of the pressure differences and for the original 6-hourly values (see section 1), using a Gaussian averaging radius r_W=250 km, aproximately the smallest r_W over which GRACE will provide useful hydrological estimates.

4. Results

4.1. RMS Differences of the 30-day Averages

Sample time series of observed data and interpolated analyzed fields are shown in Figure 4 for two sites in the United States, one in a low relief area and one in a
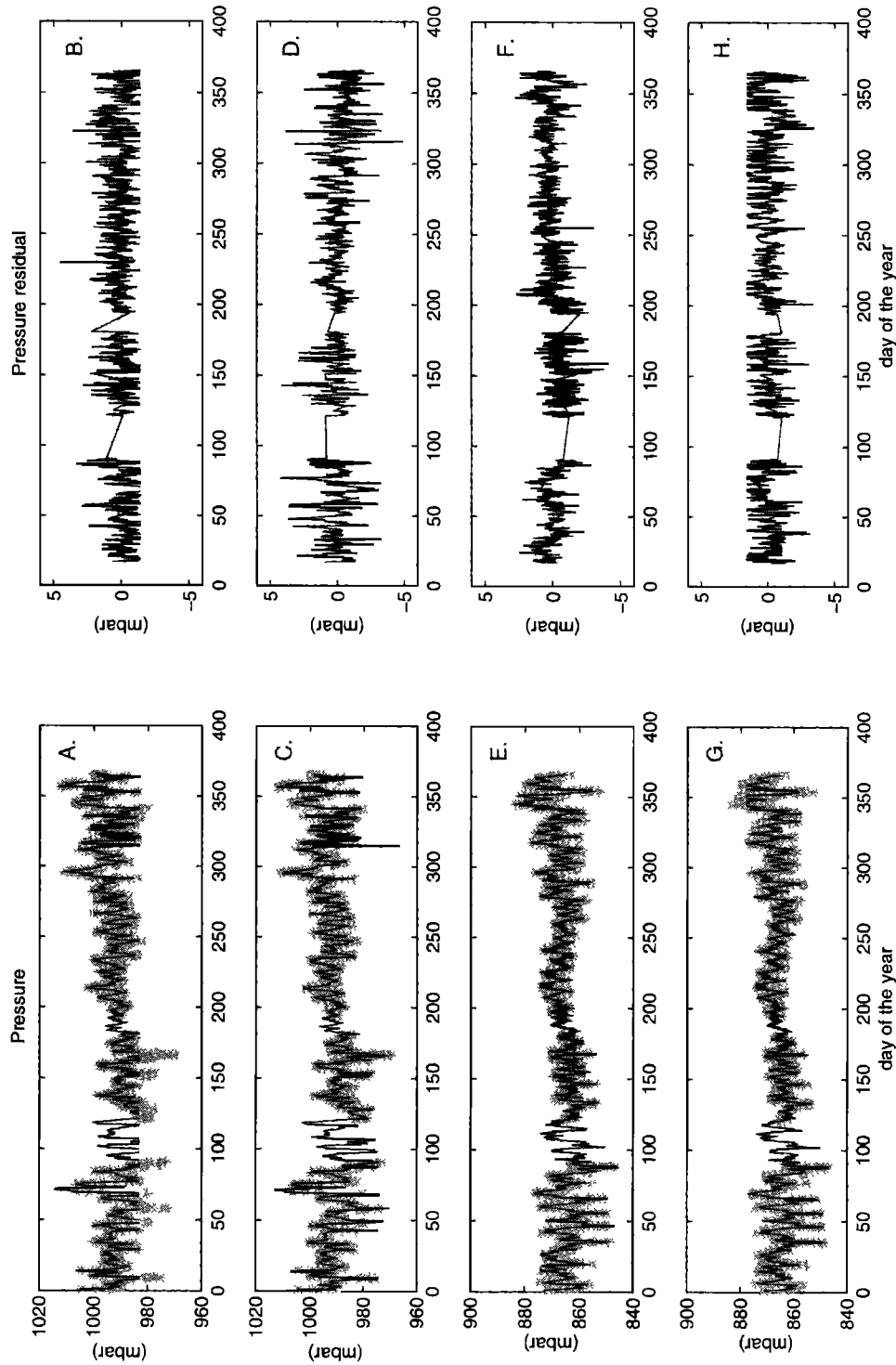
Figure 4. (a-d) Time series of surface pressure in a low-relief area (Illinois): (a) Observed (shaded stars) and interpolated ECMWF (solid line) surface pressure, (b) residual of ECMWF minus observed with means removed, (c) observed and interpolated NCEP/NCAR Reanalysis surface pressure, and (d) residual of NCEP/NCAR minus observed with means removed. (e-h) Time series of surface pressure in a high-relief area (Nevada): (e) observed (shaded stars) and interpolated ECMWF (solid line) surface pressure, (f) residual of ECMWF minus observed with means removed, (g) observed and interpolated NCEP/NCAR Reanalysis surface pressure, and (h) residual of NCEP/NCAR minus observed with means removed.
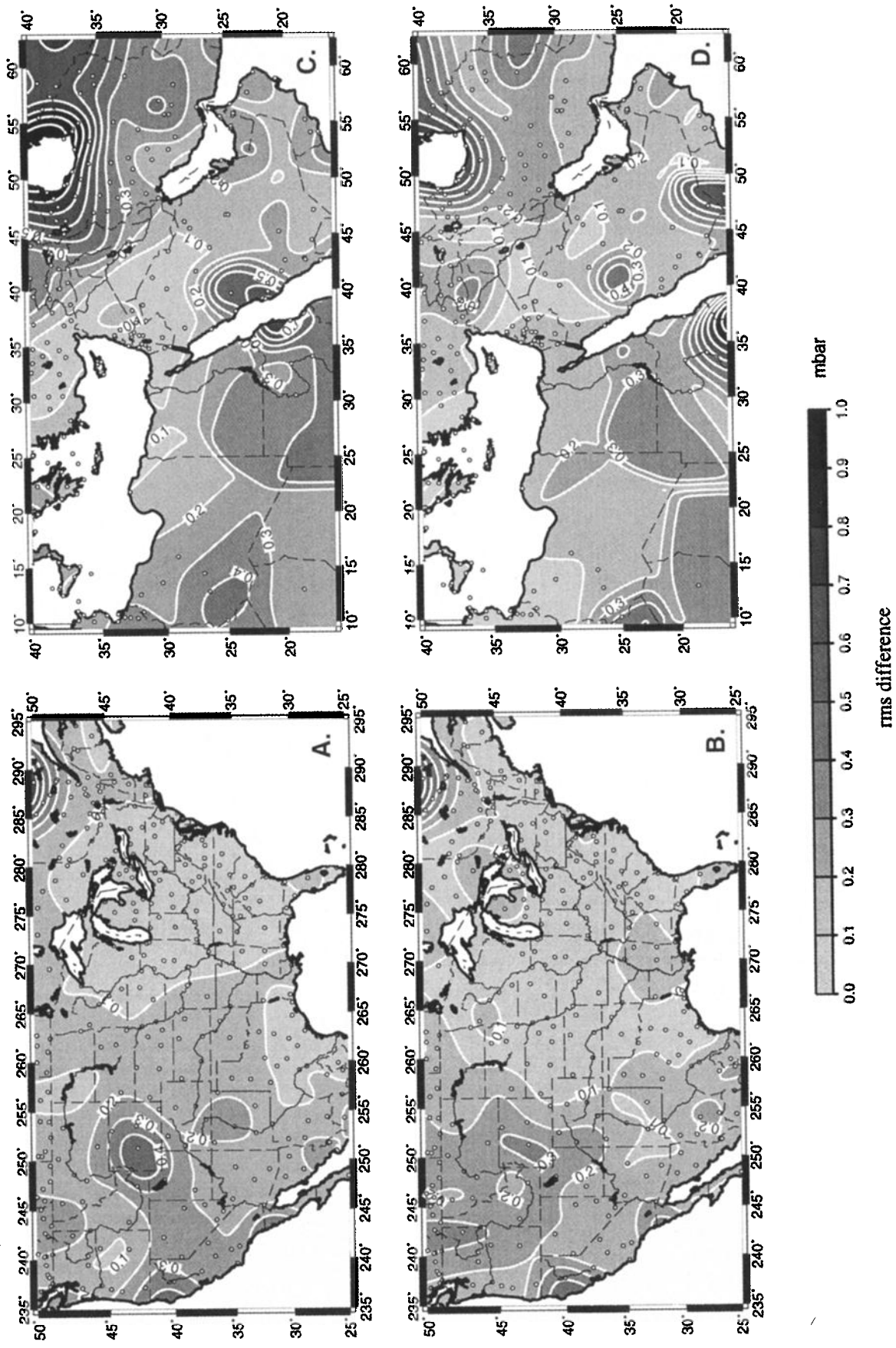
Figure 5. RMS difference of analyzed surface pressure and barometric measurements for 30-day averaging, calculated at the barometer locations. Circles are barometer locations. Dashed lines are state boundaries. (a) ECMWF in the United States. (b) NCEP/NCAR Reanalysis in the United States. (c) ECMWF in North Africa/Arabian peninsula. (d) NCEP/NCAR Reanalysis in North Africa/Arabian peninsula.

mountainous region. Figure 4 demonstrates the generally good agreement between the time series. The RMS values of 30-day averages of these differences, computed after removing the temporal mean, are contoured for the United States in Figure 5a and b for ECMWF and NCEP/NCAR analyzed fields, respectively. The RMS difference is generally < 0.2 mbar in low-relief areas for both ECMWF and NCEP/NCAR data and larger in areas of high elevation. Larger RMS is expected at high elevation because the coarse spatial resolution of the models (> 100 km) is inadequate to resolve complex orographic effects on temperature, humidity, and pressure and because (6) could be problematic for large vertical adjustments.

Figures 5c and 5b depict the RMS differences for the 30-day averages over North Africa/Arabian peninsula. In this area the distribution of barometers is much less dense than over the United States, and the observations often contain large gaps. This partially explains the RMS > 0.3 mbar in low-relief southern Egypt. Otherwise, differences in low-lying areas are generally ∼ 0.2 mbar for both ECMWF and NCEP/NCAR, except where observations are particularly sparse and in the mountainous regions of the Turkish-Iranian Plateau.

One of the problems with the comparison depicted in Figure 5 is that the ECMWF and NCEP/NCAR analyzed pressure fields are not independent of the surface pressure observations we are comparing them with. By calculating the RMS difference at the barometer location, we are comparing to assimilated observations at the point where they have been assimilated. Consequently, the comparison does not necessarily reflect the accuracy of the analyzed fields where there are no nearby observations to assimilate, and we expect the RMS difference calculated at the barometer locations to approximate a lower bound estimate of the error in the analyzed fields.

To estimate the error in the analyzed pressure fields where there are no assimilated barometric measurements, we also interpolated surface pressure observations to the grid discretization of the analyzed fields. The analyzed fields "interpolate" the pressure measurements using the governing equations of atmospheric circulation and with the aid of other data sets (including radiosonde profiles and wind velocities, which are a sensitive indicator of the pressure gradient). Hence the analyzed fields should produce a very different (and, ideally, much more accurate) "interpolation" of the assimilated barometric measurements than the simple Lagrange polynomial we have used here. Consequently, by interpolating barometric observations to the model grid and then comparing, we should get an upper bound estimate of the error in the analyzed fields consisting of the true error plus differences due to sampling limitations and interpolation error. The interpolation was done in essentially the same manner as that from the model grid to the barometer locations, except that the temperature

at each barometer site (needed for the vertical reduction in (6)) was first interpolated and reduced from the analyzed fields.

There are other reasons why this comparison is expected to overestimate the true error in the analyzed field. For example, there are gaps in the observed time series (e.g., Figure 4), whereas the analyzed field time series were complete. Consequently, if at time t, one (or more) of the four nearest barometers had no pressure measurement, the next nearest barometer was used, potentially resulting in interpolation over very large distances. Moreover, errors in the reduction and interpolation that were bias errors going from the model grid to the barometers (and hence were removed by removing the means) are not necessarily bias errors in the interpolation of barometers to the model grid because different stations are used for the interpolation at different times during the year.

Hence, by interpolating in both directions we are able to approximate both a lower bound and an upper bound estimate of error. If the observations are error-free (see the discussion in section 5), the true error should lie between these two estimates. Figure 6a and 6b show the RMS difference evaluated at the model discretization for the 30-day averages of the ECMWF and NCEP/NCAR analyzed field, respectively, in the United States. Comparing Figures 6a and 6b with Figures 5a and 5b, we note that values in Figures 6a and 6b are generally larger but mainly < 0.2 mbar in the low-relief areas for both ECMWF and NCEP/NCAR Reanalysis. The RMS difference is larger near the coastlines and at the margins of the map because the mean interpolation distance increases near the edge of barometric coverage. For North Africa/Arabian peninsula the results of the comparison at the model grid points are summarized by a map average in Table 1 (Table 2 contains similar averages for the United States). The map averages for comparisons at the model discretization are 40–90% larger than for comparisons at the barometer locations.

The RMS errors between 30-day averages of ECMWF and of NCEP/NCAR are shown in Figures 7a and 7b. In the United States (Figure 7a) the RMS errors are low, < 0.1 mbar, in low-relief areas. The RMS errors from the analyzed fields (Figure 7a) are substantially less than the RMS differences between the models and observations (Figures 5a and 5b and 6a and 6b), indicating either that the errors in the ECMWF and NCEP/NCAR analyzed fields are not entirely independent or that there are nonnegligible errors in the barometer observations. Also, the altitude difference between grids is less than between grid and observations, so part of the reduction of error could result from a decreased contribution of error introduced by vertical adjustment using (6). However, we will show in section 4.3 that this contribution is unlikely to exceed a few tenths of a millibar. Figure 7c shows the RMS error from the two models for North Africa/Arabian peninsula region. The RMS errors are quite low throughout the entire area.
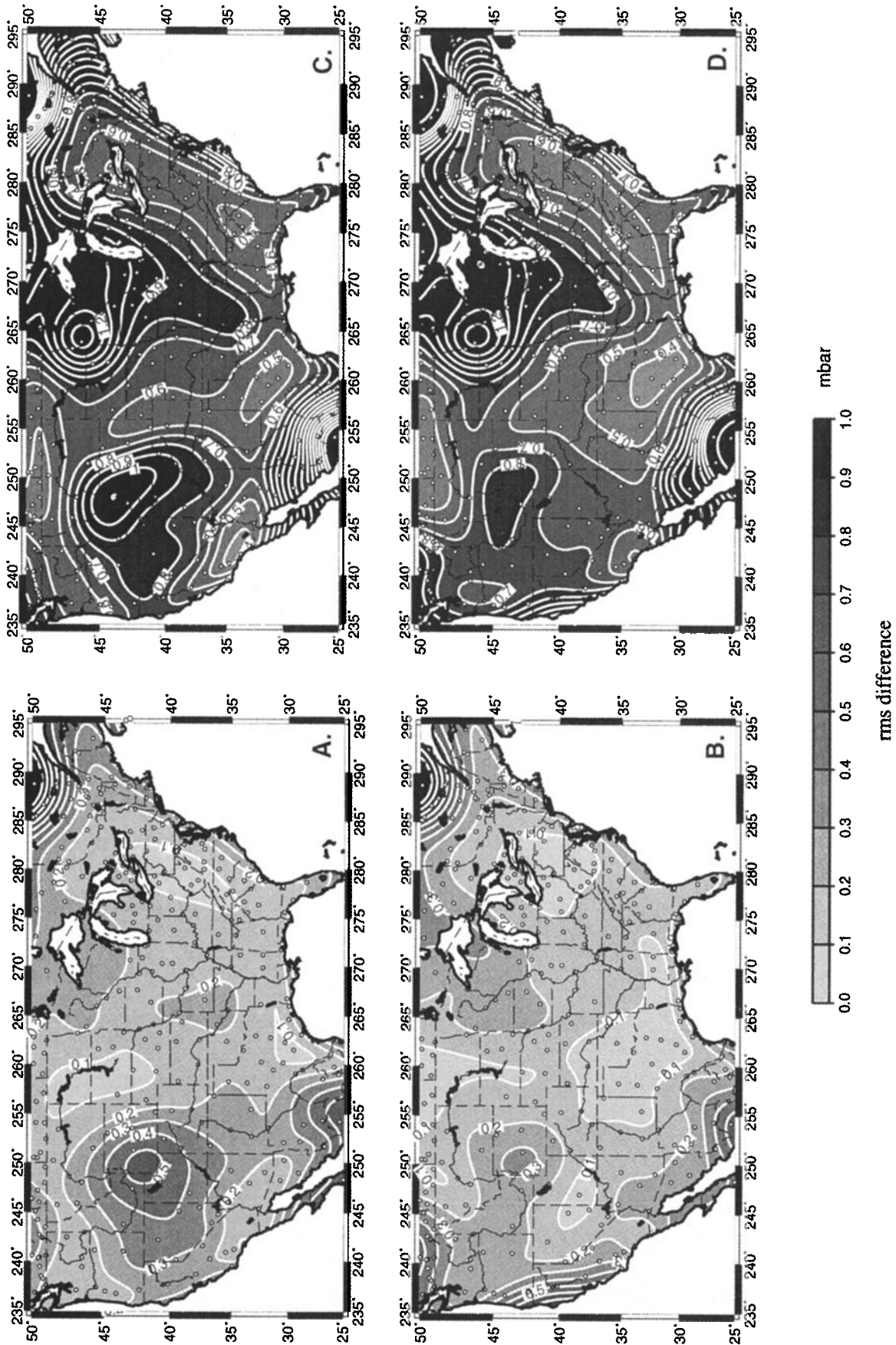
Figure 6. RMS difference of analyzed surface pressure and barometric measurements in the United States, calculated at the analyzed grid points. (a) The 30-day averaging of ECMWF; (b) 30-day averaging of NCEP/NCAR Reanalysis, (c) 6-hourly ECMWF values, and (d) 6-hourly NCEP/NCAR Reanalysis values.

Table 1. Map Averages in North Africa/Arabian Peninsula, Including the RMS Differences Calculated With Spatial Averaging and Without It.[a]

	Interpolated to Barometer Locations, mbar		Interpolated to Model Grid Points, mbar	
	Gaussian Average	No Spatial Average	Gaussian Average	No Spatial Average
30-Day Average				
ECMWF− observed	0.36	0.70	0.43	0.71
NCEP/NCAR − observed	0.26	0.62	0.48	0.63
ECMWF − NCEP/NCAR	−−	−−	0.21	0.37
NCEP/NCAR 6-hour forecast − observed	0.34	0.65	0.48	0.67
(ECMWF + NCEP/NCAR)/2 − observed	0.26	0.59	−−	−−
6-Hourly Average				
ECMWF − observed	0.91	1.32	1.29	1.86
NCEP/NCAR − observed	0.86	1.35	1.27	1.68
ECMWF − NCEP/NCAR	−−	−−	0.52	0.74
NCEP/NCAR 6-hour forecast − observed	1.33	1.70	1.61	1.98
(ECMWF + NCEP/NCAR)/2 − observed	0.79	1.21	−−	−−

[a]In the case of ECMWF-NCEP/NCAR, RMS error is used not RMS differences. For spatial averaging, see (7); $R = 250$ km.

## 4.2. RMS Differences for the 6-hourly Values

The maps in Figure 8a-8d show RMS differences between the 6-hourly values of the barometric measurements and the analyzed fields at the barometer locations with no time averaging, using a 250-km Gaussian average. These maps provide information about the short-period errors that will alias into the GRACE 30-day estimates in addition to the long-period errors ($\geq$ 60 days)

that will map directly into GRACE estimates of surface mass change. This RMS is significantly larger than the RMS of the 30-day averages shown in Figures 5a-5d. In the United States, low-relief regions typically have RMS < 0.5 mbar for both ECMWF and NCEP/NCAR data (Figures 8a and 8b). The RMS differences between the analyzed fields and observations interpolated to the model grid points (Figures 6c and 6d) are larger than

Table 2. Map Averages in the United States, Including the RMS Differences Calculated With Spatial Averaging and Without It[a]

	Interpolated to Barometer Locations, mbar		Interpolated to Model Grid Points, mbar	
	Gaussian Average	No Spatial Average	Gaussian Average	No Spatial Average
30-Day Average				
ECMWF − observed	0.17	0.59	0.26	0.53
NCEP/NCAR − observed	0.16	0.64	0.23	0.45
ECMWF −NCEP/NCAR	−−	−−	0.12	0.19
NCEP/NCAR 6-hour forecast − observed	0.34	0.71	0.35	0.53
(ECMWF + NCEP/NCAR)/2 − observed	0.13	0.58	−−	−−
6-Hourly Average				
ECMWF − observed	0.52	1.22	0.84	1.53
NCEP/NCAR − observed	0.55	1.44	0.82	1.40
ECMWF −NCEP/NCAR	−−	−−	0.37	0.57
NCEP/NCAR 6-hour forecast − observed	1.14	1.79	1.29	1.77
(ECMWF + NCEP/NCAR)/2 − observed	0.46	1.21	−−	−−

[a]In the case of ECMWF-NCEP/NCAR, RMS error is used not RMS differences. For spatial averaging, see (7); $R = 250$ km.
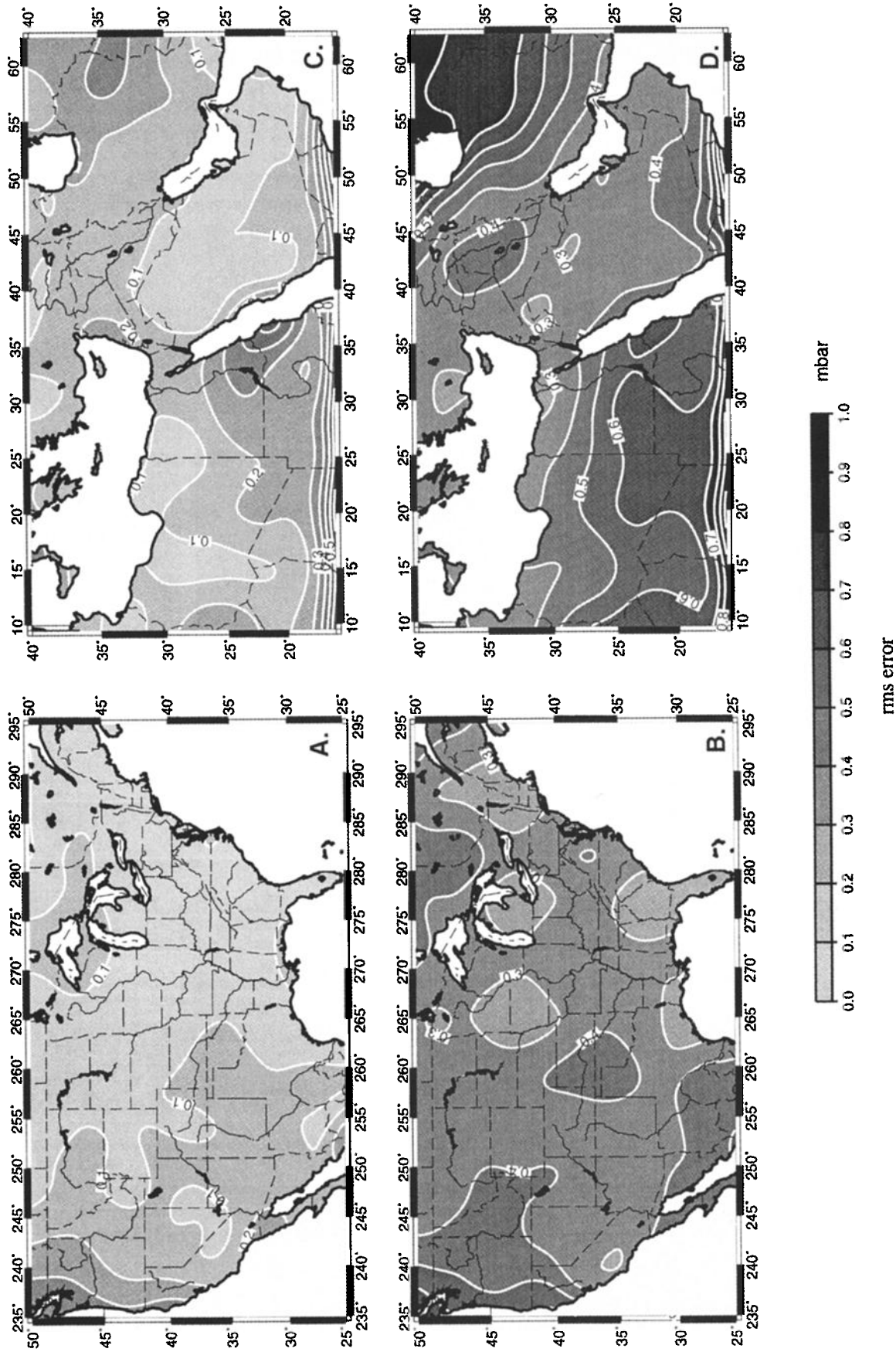
Figure 7. RMS error of ECMWF and NCEP/NCAR Reanalysis, calculated as the difference between the two fields, divided by $\sqrt{2}$. (a) The 30-day averaging in the United States, (b) 6-hourly averaging in the United States, (c) 30-day averaging in North Africa/Arabian peninsula, and (d) 6-hourly averaging in North Africa/Arabian peninsula.
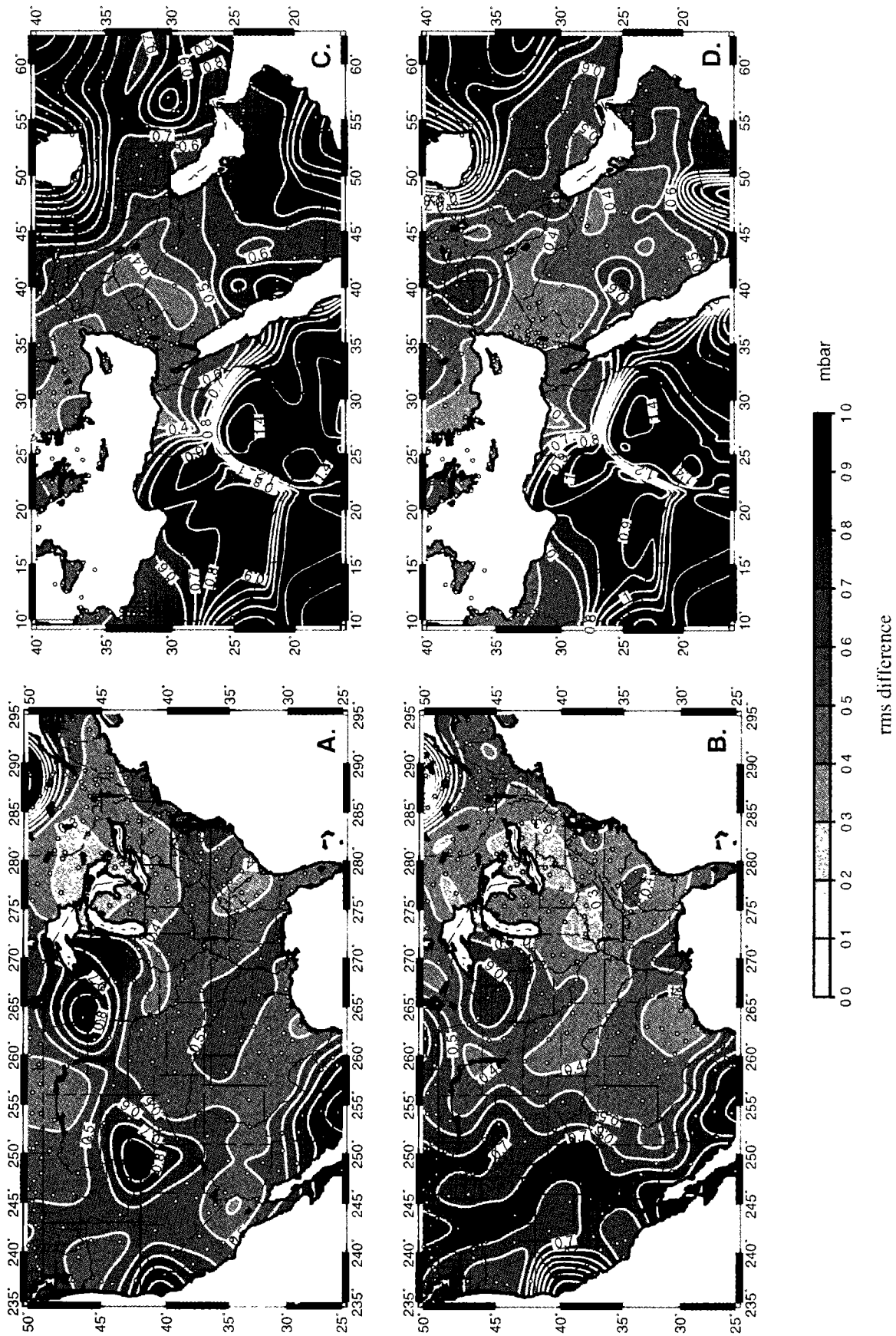
Figure 8. Rms difference between analyzed surface pressure and barometric measurements, calculated at the barometer locations. (a) The 6-hourly ECMWF values in the United States, b. 6-hourly NCEP/NCAR Reanalysis values in the United States, (c) 6-hourly ECMWF values in North Africa/Arabian peninsula, and (d) 6-hourly NCEP/NCAR Reanalysis values in North Africa/Arabian peninsula.

in Figures 8a and 8b but they are generally < 1 mbar, except in the Great Lakes region. Figures 8c and 8d depict RMS ~ 0.5 mbar in the Arabian peninsula for the NCEP/NCAR pressure field and slightly larger values for ECMWF. Large RMS (> 1 mbar) in Africa probably reflects the sparse barometer distribution and gaps in the timeseries. Table 1 gives map averages for the comparisons at the model grid points, which are 20–50% larger than those of the comparisons at the barometer locations. The RMS error of the 6-hourly fields of the two models (Figure 7d) is generally smaller.

4.3. Error Sensitivity Analysis

We expect that some fraction of the differences we have found between the observations and the analyzed fields is due to interpolation error, which would cause our RMS differences to overestimate the true error in the analyzed fields. In this section we discuss some of the possible sources of interpolation error for the particular case of interpolation from the analyzed field to the barometer locations. The sources of error that arise when interpolating the observations to the model grid points are similar.

Elevation reduction using (6) requires known elevations for the barometers and analyzed field grid. Errors in the elevations of the analyzed pressure fields are largely irrelevant because the model uses those elevations in its calculations of surface pressure, but catalogued elevations of the barometer sites can be significantly erroneous. We checked the barometer elevations by inverting (6) to solve for the elevation that best fit the pressure difference from the nearest model points, and we rejected those sites that differed by >20 m from the catalog elevation (<10 out of >400 sites were rejected). A sensitivity analysis of the error introduced by an incorrect elevation reduction indicates that a 500-m error in station elevation can increase the RMS with mean removed by as much as 1.3 mbar, whereas a 20-m error would increase the RMS by ≤ 0.02 mbar.

In addition to the elevation change, (6) also depends on the surface air temperature. Different temperature fields were used for the two models: for the NCEP/NCAR data we used the model temperature at 40 m above the ground surface, whereas for ECMWF we used a 2-m air temperature (because the 40-m temperature field was not available to us on the same grid discretization as the pressure field). Note that the 40-m air temperature is more appropriate for adjustment of the surface pressure to a new elevation using (6) because the 2-m surface temperature is subject to noise due to boundary layer effects over continents.

Sensitivity analysis of the error introduced by using an erroneous temperature field indicates that a bias error in temperature produces negligible change in the pressure RMS but that random errors can have a more significant effect. Random errors in the temperature field of up to 10°K will produce negligible changes in the

RMS of the pressure if the elevation of the measurement station is within ~ 200 m of the mean elevation of the nearest model grid points. However, when the station elevation differs by > 200 m from the weighted mean model elevation (as commonly occurs in mountainous regions), random errors in the temperature field of the order of 1°K can influence the pressure correction significantly.

For example, the station at Table Mountain Gravity Observatory (TMGO) near Boulder, Colorado, is ~500 m lower than the weighted mean of the nearest ECMWF grid points. A 1.5°K RMS temperature error at those grid points would produce a 0.2 mbar RMS pressure error in the interpolation of pressure to TMGO. Boundary layer effects can cause 2-m and 40-m estimates of air temperature to differ by 1.5°K RMS for the 6-hourly values. Consequently, the 6-hourly values of interpolated pressure from ECMWF and NCEP/NCAR may differ by a few tenths of a millibar solely because of the different temperature levels used. However, the 0.2-mbar error that might be attributed to the elevation reduction represents only ~15% of the total 1.35-mbar RMS difference of the 6-hourly time series at TMGO. Consequently, most of the RMS difference at TMGO consists of a real discrepancy between the analyzed field and barometric measurements, rather than errors in the interpolation/reduction of the model pressure to the station location. Note also that the Gaussian averaged RMS difference between models and observations in the vicinity of TMGO (Figure 8a) is much less than 1.35 mbar; this is because Gaussian spatial averaging reduces differences due to pressure variations on short spatial wavelengths. This can also be seen by comparing the "No Spatial Averaging" columns in Tables 1 and 2 with the "Gaussian Average" columns.

Pressure in (6) also depends on the specific humidity Q because T is in fact an approximation for $T(1 + 0.6078Q)$ [Gill, 1982]. The error introduced by the implicit assumption that $Q = 0$ could introduce up to 3°K RMS difference in equivalent temperature. Hence we expect that in low-relief areas the error introduced by variable Q is negligible, but in areas with high relief this can add several tenths of a millibar to the pressure RMS. To further test the dependence on specific humidity, we calculated RMS differences using $T(1+0.6078Q)$ and surface Q from the analyzed fields. In low-relief areas the RMS differences changed negligibly from those using just T, but in high-relief regions they were actually slightly larger after correcting for Q. Given that water vapor in the atmosphere can change significantly on scales of a few kilometers, this would suggest that the model discretization is too coarse to adequately constrain Q for purposes of altitude correction using (6). We also examined the effect of a variable lapse rate. An empirical relation between lapse rate and temperature can be used in place of the 6.5°K kilometers^{-1} lapse rate in (6) [Manabe and R. Wetherald, 1967]. The
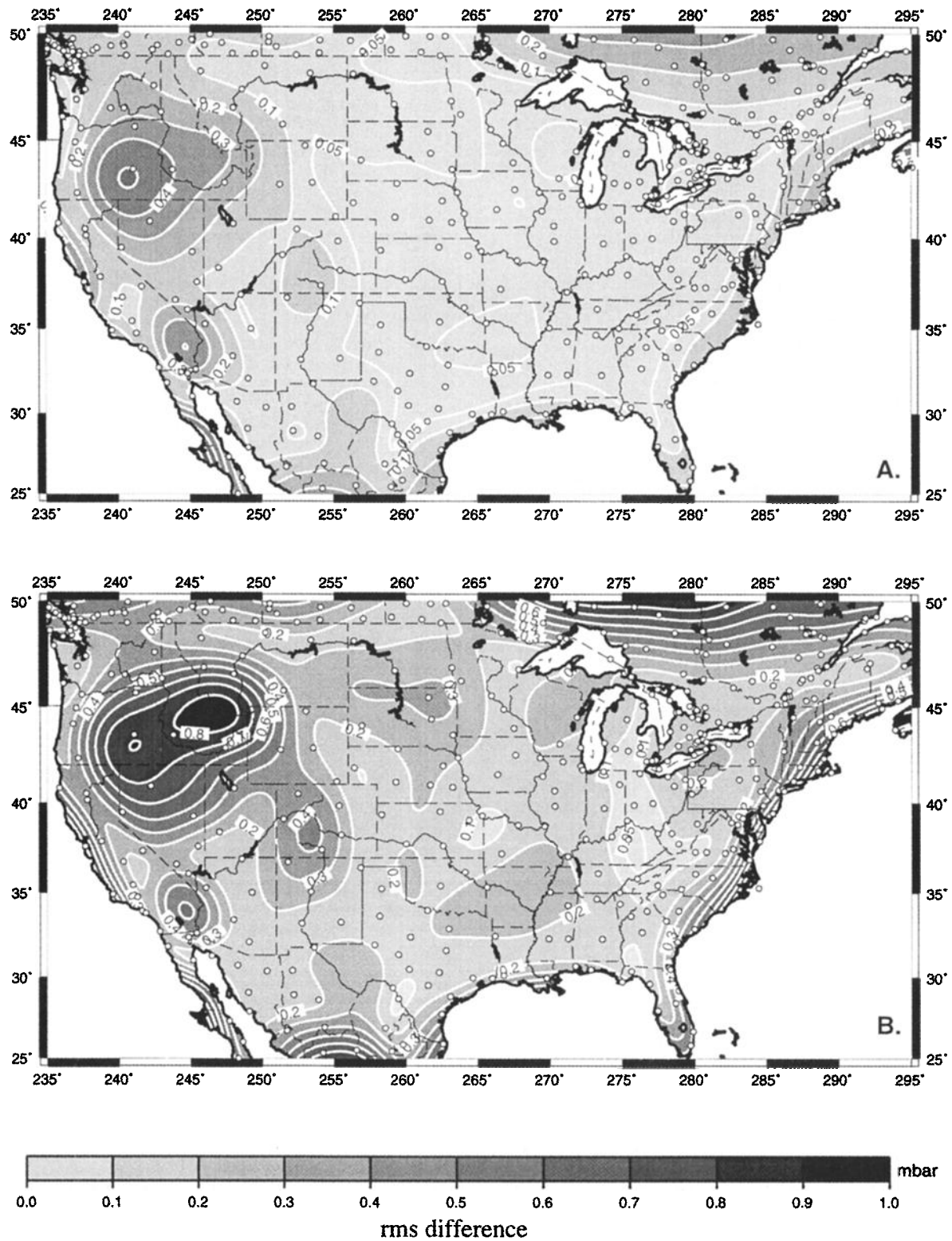
Figure 9. Rms difference between the ECMWF and synthetic "observation" data sets in the United States. (a) The 30-day averages and (b) 6-hourly averages.

change in RMS pressure difference was negligible (averaging <0.01 mbar).

From this sensitivity analysis we conclude that errors introduced by interpolation of the analysis field to the barometer locations are negligible. In the worst case (i.e., using 2-m air temperature for reduction in high-relief regions) the contribution to the RMS difference is a few tenths of millibar, and so these errors can be neglected.

4.4. Surface Pressure Field From Barometric Measurements

An alternative means of removing the atmospheric mass contribution from the gravity field delivered by GRACE would be to use the barometric measurements themselves to estimate the large-scale pressure variations, particularly in regions (e.g., Antarctica) where the accuracy of the analyzed pressure fields is suspect [*Wahr et al.*, 1998]. To assess the accuracy of surface pressure fields reconstructed from surface pressure measurements, we created a synthetic "observed" data set by interpolating the ECMWF analyzed pressure fields to the barometer locations. Then we interpolated both the original ECMWF fields and the ECMWF expressed at the barometric sites to a regular grid with ETOPO5 elevations [*Row et al.*, 1995]. The RMS differences for the 30-day averages in the United States are small, < 0.1 mbar, with slightly larger values in the Rocky Mountain regions, ~ 0.3-0.5 mbar (Figure 9a). The RMS differences for the 6-hourly values (Figure 9b) are also small, < 0.3 mbar in low-relief areas and < 0.9 in mountainous areas. Thus with an adequate barometer distribution it would be possible to reduce the atmospheric contamination of GRACE hydrology estimates to the equivalent of just a few millimeters of water. However, this comparison is perhaps overly optimistic in that it assumes no gaps in data. Also, if we were to instrument poorly constrained areas of the globe, perhaps a better alternative to using the pressure measurements directly would be to let NCEP and/or ECMWF incorporate the measurements into their operational database for assimilation into the analyzed fields and hence improve the models in those regions.

5. Discussion and Conclusions

The accuracy with which GRACE can map the Earth's gravity field is limited by several sources of error, including system noise error in the satellite-to-satellite microwave ranging measurements, accelerometer error, error in the ultrastable oscillator, and orbit error. The accuracy depends somewhat on the orbital configuration (on the altitude and spacecraft separation, for example). However, system design is such that the atmospheric mass correction represents the limiting factor when using GRACE measurements to infer changes in water storage on land at wavelengths of ~300 km and larger [*Wahr et al.*, 1998].

Errors in estimation of surface pressure result in errors in the GRACE hydrology estimates that will lie somewhere between two end-member contributions. If we assume that there is no aliasing, so that atmospheric pressure errors at periods < 60 days are nullified by GRACE averages, then we need only consider the errors in the 30-day averages of the pressure fields. This is end-member 1. The effect of aliasing high-frequency variations into the GRACE solution is more complicated. A short-period pressure error aliased into the GRACE 30-day averages can affect locations well outside the region where the pressure error was located. These aliasing errors are apt to be smaller than the short-period pressure error because some of that error will indeed be averaged out over each 30-day period. However, for end-member 2 we cannot rule out the worst case scenario that averaging is ineffective, and the RMS error of the 6-hourly pressure fields will be fully aliased into the 30-day hydrology estimates.

The largest source of uncertainty in our error estimates derives from the fact that most of the pressure measurements used for comparison were also assimilated into the analyzed fields. Comparisons where the analyzed fields are interpolated to the locations of the assimilated barometric measurements (the "lower bound" estimate) may underestimate the true error because the RMS differences do not reflect possible errors in regions where there are no nearby barometric measurements to constrain the pressure field. Hence we also calculate the RMS difference for the barometer measurements interpolated to the grid points of the analyzed fields, where there may not be nearby measurements (the upper bound estimate). Because the models assimilate other observations besides barometric measurements, the variance of the upper bound RMS pressure differences ought to be larger than the variance of the analyzed pressure field errors.

Errors in the barometric measurements cause our estimates to be either too large or too small, depending on the effectiveness of the assimilation. For example, suppose the barometric measurement error is large relative to the error in the analyzed fields and that the assimilation of pressure measurements changes the analyzed surface pressure fields negligibly. Then the difference between the analyzed fields and measurements will predominantly represent errors in the measurements, and our estimates of the errors in the analyzed fields will be inflated. On the other hand, suppose the assimilation is highly effective, so that the analyzed pressure fields are forced to agree closely with the pressure observations. The analyzed field would be forced toward the erroneous values at measurement sites, and the errors would be common to both the analyzed field and the observation, so they would not show up in the difference. In this case, the difference would underestimate the true error in the analyzed field. This latter possibility that the error is underestimated most concerns us here.
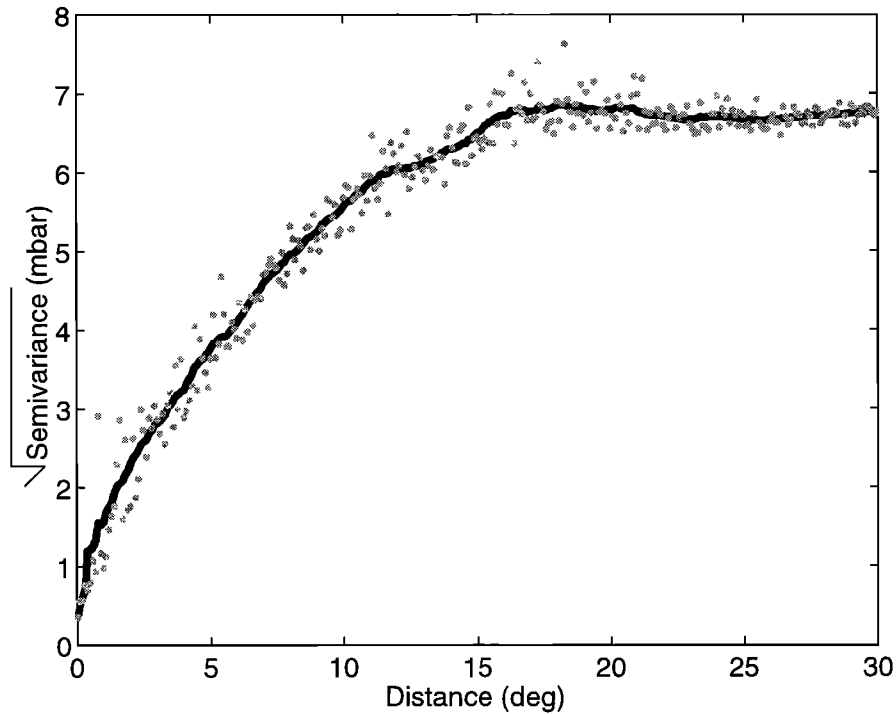
Figure 10. Square root of the semivariance of pressure measurements for the United States in 0.1° bins (shaded dots) and smoothed (solid line).

There are two potential contributions to observational error. One can be loosely termed as measurement error. This includes, of course, errors in the barometric measurements themselves. Most present-day barometers provide short-term accuracies of 0.08 mbar and have long-term stabilities of 0.1 mbar yr^{-1}, with overall uncertainties estimated to be ±0.15 mbar (C. Conquest, personal communication, 2000). Unfortunately, there can be other forms of measurement error, including timing errors where measurements are made slightly offset to 0000, 0600, 1200, or 1800 UT but are assimilated as though they were made at exactly one of those times (e.g., surface measurements by radiosondes, which comprise 20% of our stations, are sometimes collected a few hours after the targeted time if there is thunderstorm activity or equipment failure).

To independently assess the measurement error amplitude, we constructed a spatial semivariance function from the pressure measurements. The spatial semivariance is one half the mean square difference between measurements as a function of spatial separation (as contrasted with the temporal semivariance used earlier for outlier removal, which is the mean square difference as a function of elapsed time). To estimate the spatial semivariance, we paired each barometric station in the United States with every other station, binned the station pairs according to angular distance between stations in 0.1° (~11 km) incremental bins, reduced the pressures of one station to the elevation of the other using (6), and summed the squared difference of all simultaneous measurements for all station pairs in the

bin. The square root of the resulting estimate of semivariance is shown in Figure 10.

Note from Figure 10 that the semivariance is approximately independent of distance (i.e., uncorrelated) for angular distances greater than ~15°. At large separations the root semivariance converges to the RMS of surface pressure over the United States. That large-distance limit is between 6.5 and 7 mbar. The semivariance decreases with decreasing station separation because the closer two stations are to one another, the more correlated their pressure records will be.

In the limit of two stations at the same location the root semivariance simply reflects the measurement error. Figure 10 indicates that station pairs spaced <0.4° apart have root semivariance <0.7 mbar (10% of all U.S. radiosonde sites and 8% of all other U.S. barometer locations are within 0.4° of another United States barometer). Also in Figure 10, the root semivariance appears to intercept the y axis (corresponding to zero station separation) at no more than a few tenths of a millibar. This suggests that measurement errors, including the timing errors from radiosondes, are indeed of the order of a few tenths of a millibar or less. Furthermore, this is an estimate of the measurement error at a single station and for a single 6-hourly value. The effects on the GRACE Gaussian averages should be smaller, and the 30-day averages should reduce even further (compare, for example, the values shown in the 6-hourly, No Spatial Averaging columns in Tables 1 and 2 with the much smaller values shown in the 30-day average, Gaussian Average columns).

A second potential source of error in the pressure observations would be fine-scale spatial variability in the pressure field at wavelengths shorter than can be described by either the barometer distribution or the analyzed fields. Scales this short would be finer than needed to correct GRACE data but might still be coarse enough that a point measurement obtained with a barometer might be partially unrepresentative of the pressure field at the scale of the model grid. Short-scale pressure variations would be aliased into larger-scale pressure variation of the analyzed field, and the resulting errors would not show up in differences between the analyzed field and barometric measurements.

Possible contamination by short-scale variability caused us to examine one other approach, standard in meteorology, for estimating the absolute maximum error in the analyzed fields: comparing the barometric measurements with 6-hour forecast fields. The 6-hour forecasts use the complete set of three-dimensional analyzed fields from time $t-(6$ hours) as initial conditions, then propagate those fields forward to time t using the dynamical equations of the atmosphere. The input analyzed fields assimilate observations taken at time $t-(6$ hours), but the resulting forecast field does not depend in any way on measurements taken at time t. This comparison will overestimate the "true" error in the analyzed fields, both because the analyzed fields at time t are certainly improved by the assimilation of observations taken at time t and because the observational errors (which are presumably uncorrelated with the errors in the forecast fields) will contribute directly to the differences.

We examined only the NCEP/NCAR 6-hour forecast fields because the ECMWF forecasts were not available to us. The map averaged RMS difference for comparison at the barometer locations is 0.34 mbar for the 30-day RMS difference and 1.14 mbar for the 6-hourly RMS difference over the United States, and 0.34 mbar and 1.33 mbar, respectively, for North Africa/ Arabian peninsula. Tables 1 and 2 also give the results of comparison at the model grid points.

All of the Gaussian-averaged, 30-day RMS pressure differences given in Tables 1 and 2 indicate that the analyzed fields will be adequate to remove the atmospheric contribution to GRACE estimates of surface hydrological mass changes to an accuracy of better than 0.5 cm of equivalent water thickness. The comparisons of 6-hourly fields yield larger RMS differences of between 0.5 and 1.6 mbar. The relevance of the 6-hourly values for GRACE, however, remains unclear. A detailed orbital simulation is required to clarify the temporal-aliasing effects of short-period atmospheric error. In any case, one should note that all of the results presented here are for data from 1998. The accuracy of global circulation models will likely have improved by the time of GRACE launch. We also note that previous estimates of error in the analyzed pressure fields [*Wahr et al.*, 1998] based on the difference between ECMWF

and NCEP pressure fields significantly underestimate the true error because errors in these two fields are partially correlated. We considered ways in which the atmospheric correction to GRACE data might be improved, including averaging together the pressure fields from ECMWF and NCEP/NCAR, which should reduce uncorrelated errors present in the two fields. Comparisons of (ECMWF+NCEP/ NCAR)/2 to the barometric measurements are given in Tables 1 and 2. The improvement is very slight (0-18% over the better of the two RMS differences) because most of the error in the analyzed fields is correlated.

Another conclusion of this paper is that if the distribution of barometers is sufficiently dense, then pressure measurements can be used independently of analyzed pressure fields to correct for the effects of atmospheric mass variability. Our analysis suggests the United States barometer network would be capable of delivering 30-day Gaussian-averages of surface pressure to an accuracy that is everywhere better than 0.5 mbar. However, the interpolation of ECMWF used to reconstruct the pressure field from synthetic "measurements" may give misleading results because short-scale variability in real pressure observations could be erroneously aliased into pressure fields reconstructed from such observations. Hence we also calculated the error from kriging interpolation of the barometric measurements to the model grid points. Kriging uses the semivariance properties of a field to estimate the optimal interpolation [*Davis*, 1986]. The error in interpolated values can be estimated as the dot product of the interpolation weights with the semivariance at the corresponding distances. We used the square of the smoothed root semivariance shown as the solid line in Figure 10 and found that the average interpolation error in the United States was 0.75 mbar. This error estimate implicitly incorporates the measurement error (including timing errors), the errors related to aliasing of fine-scale spatial variations in pressure, and the error due to gaps in the measurement time series. Furthermore, this 0.75 mbar error represents map-averaged error in the interpolated 6-hourly value at a single point. The error in 30-day Gaussian averages would be substantially smaller.

Reconstruction of pressure fields from measurements could be particularly useful for regions (e.g., Antarctica) where analyzed fields are particularly inaccurate, although the barometric networks in those regions are apt to be far less dense than in the United States. With 0.4 barometers per 10,000 km^2 area, it should be possible to obtain an accuracy of ~1 mbar. This approach might be suitable for postprocessing of GRACE data in regions where national or local barometric data are not real-time telemetered and so cannot be incorporated into the operational databases of the analyzed fields.

References

Chao, B.F., and R.S. Gross, Change in the Earth's rotation and low-degree gravitational field introduced by earthquakes, *Geophys. J. R. Astron. Soc., 91,* 569-596, 1987.

Chao, B.F., W.P. O'Connor, A.T.C. Chang, D.K. Hall, and J.L. Foster, Snow-load effect on the Earth's rotation and gravitational field, 1979-1985, *J. Geophys Res, 92,* 9415-9422, 1987.

Davis, J.C., *Statistics and Data Analysis in Geology, 2nd ed.,* pp. 239-248, Wiley and Sons, New York, 1986.

Dickey, J.O., et al., *Satellite Gravity and the Geosphere,* 112 pp., Natl. Acad. Press, Washington, D.C., 1997.

European Centre for Medium-Range Weather Forcasts (ECMWF), The description of the ECMWF/WCRP level IIIA global atmospheric data archive, Data Services publication, Reading, England, 1995.

Gill, A.E., *Atmosphere-Ocean Dynamics,* pp. 40-41, Academic, San Diego, Calif., 1982.

Haurwitz, B., *Climatology,* p. 12, McGraw-Hill, New York, 1941.

Jekeli, C., Alternative methods to smooth the Earth's gravity field, *Rep. 327,* Dept. of Geod. Sci. and Surv., Ohio State Univ., Columbus, 1981.

Kalnay, E., et al., The NMC/NCAR 40-year reanalysis project, *Bull. Am. Meteorol. Soc., 77,* 437-471, 1996.

Kaula, W.M., Global harmonic and statistical analysis of gravity, in *Extension of Gravity Anomalies to Unsurveyed Areas,* edited by H. Orlin, *Geophys. Monogr. Ser.,* vol. 9, edited by H. Orlin, pp. 58-67, AGU, Washington, D.C., 1966.

Manabe, S., and R. Wetherald, Thermal equilibrium of the atmosphere with a given distribution of relative humidity, *J. Atmos. Sci, 24,* 241-259, 1967.

Neibauer, T.M., and J.E. Faller, Continuous gravity observations using Joint Institute for Laboratory Astrophysics absolute gravimeters, *J. Geophys Res, 97,* 12,427-12,435, 1992.

Rocken, C., R. Ware, T. van Hove, F. Solheim, C. Alber, and J. Johnson, Sensing atmospheric water vapor with the Global Positioning System, *Geophys. Res. Lett., 20,* 2631-2634, 1993.

Row, L.W., D.A. Hastings, and P.K. Dunbar, TerrainBase Worldwide Digital Terrain Data, documentation manual, [CD-ROM], release 1.0, Natl. Geophys. Data Center, Boulder, Colo., 1995.

Van Dam, T., G. Blewitt, and M.B. Heflin, Atmospheric pressure loading effects on Global Positioning System coordinate determinations, *J. Geophys Res, 99,* 23,939-23,950, 1994.

Wahr, J., M. Molenaar, and F. Bryan, Time-variability of the Earth's gravity field: Hydrological and oceanic effects and their possible detection using GRACE, *J. Geophys. Res., 103,* 30,205-30,230, 1998.

I. Velicogna and J. Wahr, Department of Physics and Cooperative Institute for Research in Environmental Science, Campus Box 390, University of Colorado, Boulder, CO 80309-0390. (isabella@colorado.edu; wahr@colorado.edu)

H. M. Van den Dool, Climate Prediction Center, National Centers for Environmental Prediction, 5200 Auth Road, Washington, DC 20233. (hvandendool@ncep.noaa.gov)